Electronic Supplementary Material (ESI) for Chemical Science.
This journal is © The Royal Society of Chemistry 2016

Supporting Information

Emission Color Tuning and White-Light Generation Based on Photochromic Control of Energy Transfer Reactions in Polymer Micelles

Magnus Bälter, Shiming Li, Masakazu Morimoto, Sicheng Tang, Jordi Hernando, Gonzalo Guirado, Masahiro Irie, Françisco M. Raymo, and Joakim Andréasson*

Synthesis

Experimental procedures for the preparation of **DAE** and the **ST-7-4** copolymer have been reported previously.[1, 2] 9, 10-diphenylanthracene (**DPA**) was purchased from Sigma-Aldrich and used without further purification.

Experimental Section

All micelle experiments were performed in aqueous solution (mQ). The samples were prepared by mixing amphiphilic polymer **ST-7-4** with **DPA** and **DAE** in dichloromethane and film formation was promoted by evaporation of the solvent in a vacuum chamber. The guest encapsulating micelles were formed by rehydration of the film for 10 min. with mQ-water followed by filtration with 0.25µm cellulose acetate filter. In the case of combined micelles (the cocktails containing both **DPA** and **DAE**), the **DPA** and the **DAE** samples were mixed in the adequate proportions. The average molecular weight of the individual micelles was determined to be 133 kDa based on static light scattering measurements. With a total amount of 0.4 mg **ST-7-4** used in each preparation and a 10% loss in the filtration process, the total micelle concentration was 1.35 µM.

Ground state absorption spectra were recorded on a Cary 5000 UV/vis spectrometer. Corrected fluorescence spectra were recorded on a SPEX Fluorolog-3 spectrofluorimeter. Fluorescence lifetimes were measured using a time correlated single photon counting (TC-SPC) setup. The excitation light, λ_{exc} = 377 nm, was provided at a repetition rate of 20 kHz by a 377 nm diode laser (LDH-P-C-375) powered by a PDL 800B pulsed diode driver (Picoquant, GmbH Germany). The emitted photons were collected at the magic angle (54.7°) at 400 and 530 nm alternatively by a thermoelectrically cooled microchannel plate photomultiplier tube (R3809U-50, Hamamatsu). The signal was digitalized using a multi-channel analyzer with 2048 channels (SPC-300, Edinburgh Analytical Instruments) and to ensure good statistics 10 000 counts were recorded in the top channel. The measured fluorescence decays were fitted using the program FluoFit Pro v.4 (PicoQuant GmbH, Germany) after deconvolution of the data with the instrument response function (IRF) with FWHM~40 ps.

Electrochemical details. Solvent and the supporting electrolyte: acetonitrile from SDS was used as received (water content less than 10 mg kg^{-1}). Tetrabutylammonium tetrafluoroborate and tetrabutylammonium hexafluorophosphate, as a supporting electrolyte, were of high purity and used without further purification.

Cyclic voltammetry experiments: a computer controlled VSP potentiostat (Versatile Modular Potentiostat) was used to perform the cyclic voltammetry at low scan rates in the range 0.1–1.0 V s^{-1}.

An electrochemical conical cell equipped with a methanol jacket, which makes it possible to fix the temperature at 20°C by means of a thermostat, was used for the set-up of the three electrode system. For cyclic voltammetry experiments, the working electrode was, in all cases, a glassy carbon disk of a diameter of 1.0 mm. It was polished using a 1 mm diamond paste. The counter electrode was a glassy carbon disk of 0.3 cm diameter. All of the potentials are reported vs. SCE isolated from the working electrode compartment by a salt bridge. The salt solution of the reference calomel electrode is separated from the electrochemical solution by a salt bridge ended with a frit, which is made of a ceramic material, allowing ionic conduction between the two solutions and avoiding appreciable contamination. Argon was allowed to flow under the solution during the measurements. The concentration of electroactive substances was between 1 and 10 mM while the supporting electrolyte concentration was 0.1 M.

Isomerization reactions. The photoinduced isomerization reactions of **DAE** were performed in the UV using a UVP lamp model UVGL-25 (365 nm, 1.5 mW/cm^2) or in the visible with a 5 W green LED emitter centered around 523 nm (FWHM = 40 nm) delivering a light power of 0.4 W.

For fluorescence quantum yield determinations in acetonitrile and in the micells, the reference compound used for **DPA** was **DPA** itself in cyclohexane (Φ_F = 0.97)[3] and for **DAEc** Coumarin 153 in ethanol (Φ_F = 0.54)[4] was used.

Spectral properties of DPA and DAE in acetonitrile

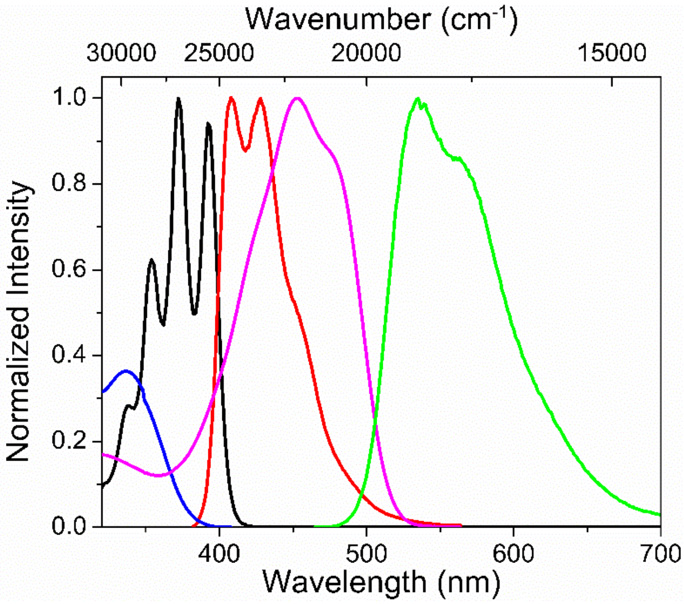

Figure S1. Absorption spectra of **DAEo** (blue line), **DAEc** (magenta line), **DPA** (black line) and emission spectra of **DPA** (red line) and **DAEc** (green line) in acetonitrile. All spectra are normalized except from that of **DAEo**, where the absorption is shown in the correct relation to **DAEc** with regard to the molar absorption coefficient.

Steady-state emission and time resolved single photon counting (SPC) data at different concentrations.

Figures S2-S7 below are organized as follows:

Left panel: Steady-state emission (λ_{exc} = 375 nm). **DPA** alone (black), **DAEc** alone (blue), and the **DPA+DAEc** cocktail (red).

Middle and right: Time-resolved (SPC) fluorescence decays of **DPA** (λ_{exc} = 377 nm, λ_{em} =400 nm) and **DAEc** (λ_{exc} = 377 nm, λ_{em} = 530 nm), respectively.

The following parameters are also determined for each set of measurements:

Quenching efficiency of **DPA** in the cocktail from steady-state measurements ($E_{quench,\ SS}$)

Quenching efficiency of **DPA** in the cocktail from SPC measurements ($E_{quench,\ SPC}$)

FRET efficiency (E_{FRET})

The average fluorescence lifetime presented in the tables (τ_{avg}) were calculated using the pre-factor weighted average of the decays. The negative pre-factors and the corresponding lifetimes, resulting from a FRET-induced risetime for **DAE**, were, of course, omitted.

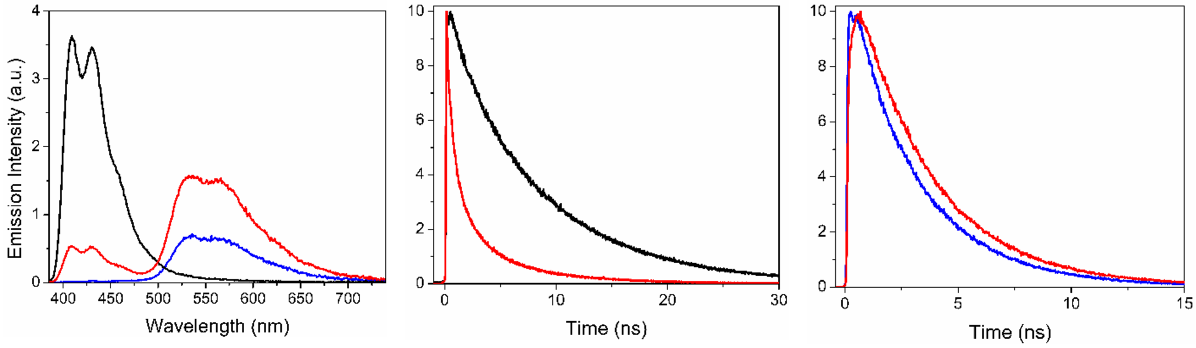

Figure S2. [**DPA**] = 0.9 μM, [**DAEc**] = 0.7 μM.

Decay	A_1	τ_1 (ns)	A_2	τ_2 (ns)	A_3	τ_3 (ns)	τ_{avg}(ns)	χ^2
DPA alone (black)	1316	8.5	250	1.5	-	-	7.4	1.05
DPA cocktail (red)	213	6.4	527	1.8	972	0.35	1.6	1.19
DAEc alone (blue)	1245	3.3	412	1.7	-	-	2.9	1.0
DAEc cocktail (red)	218	3.4	1538	3.1	-463	0.27	3.3	1.0

($E_{quench,\ SS}$) = 0.85
($E_{quench,\ SPC}$) = 0.79
(E_{FRET}) = 0.70

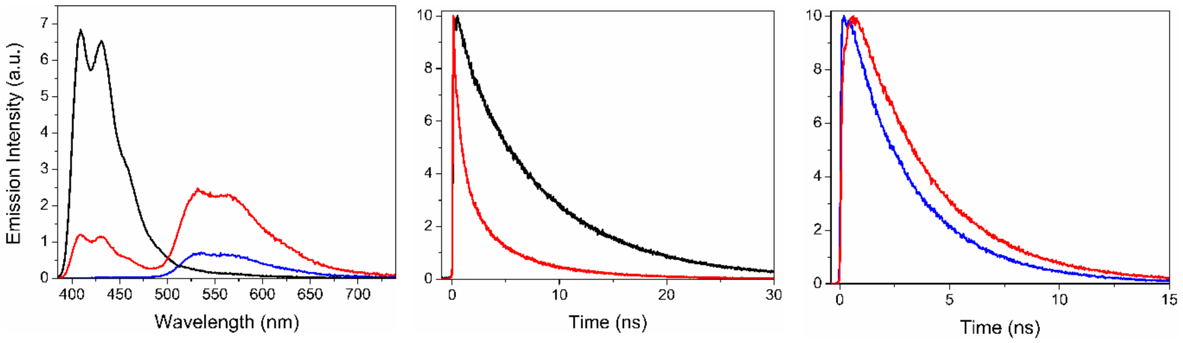

Figure S3. [**DPA**] = 1.8 μM, [**DAEc**] = 0.7 μM.

Decay	A_1	τ_1 (ns)	A_2	τ_2 (ns)	A_3	τ_3 (ns)	τ_{avg} (ns)	χ^2
DPA alone (black)	1291	8.4	276	1.5	-	-	7.2	1.09
DPA cocktail (red)	352	5.7	607	1.5	838	0.28	1.6	1.12
DAEc alone (blue)	1245	3.3	412	1.7	-	-	2.9	1.0
DAEc cocktail (red)	1792	3.5	-586	0.29	-	-	3.5	1.16

$E_{quench,\ SS} = 0.82$
$E_{quench,\ SPC} = 0.78$
$E_{FRET} = 0.74$

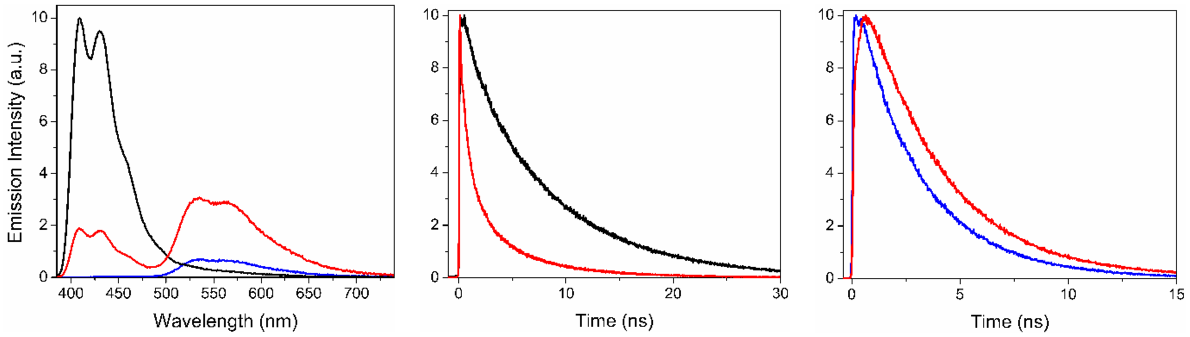

Figure S4. [**DPA**] = 2.7 μM, [**DAEc**] = 0.7 μM.

Decay	A_1	τ_1 (ns)	A_2	τ_2 (ns)	A_3	τ_3 (ns)	τ_{avg} (ns)	χ^2
DPA alone (black)	1241	8.3	340	1.3	-	-	6.8	1.12
DPA cocktail (red)	366	5.4	616	1.4	769	0.27	1.7	1.16
DAEc alone (blue)	1245	3.3	412	1.7	-	-	2.9	1
DAEc cocktail (red)	1846	3.6	-815	0.31	-	-	3.6	1.11

$(E_{quench,\ SS}) = 0.81$
$(E_{quench,\ SPC}) = 0.75$
$(E_{FRET}) = 0.71$

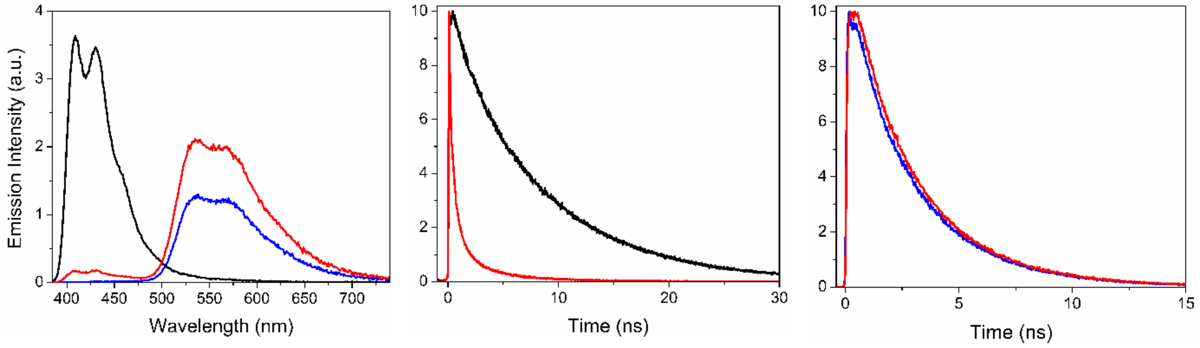

Figure S5. [**DPA**] = 0.9 µM, [**DAEc**] = 1.4 µM.

Decay	A$_1$	τ_1 (ns)	A$_2$	τ_2 (ns)	A$_3$	τ_3 (ns)	τ_{avg} (ns)	χ^2
DPA alone (black)	1316	8.5	250	1.5	-	-	7.4	1.05
DPA cocktail (red)	107	4.6	467	1.1	1288	0.20	0.66	1.27
DAEc alone (blue)	1309	3.1	333	1.2	-	-	2.7	1.0
DAEc cocktail (red)	992	3.4	693	2.0	-	-	2.8	1.0

($E_{quench, SS}$) = 0.95
($E_{quench, SPC}$) = 0.91
(E_{FRET}) = 0.59

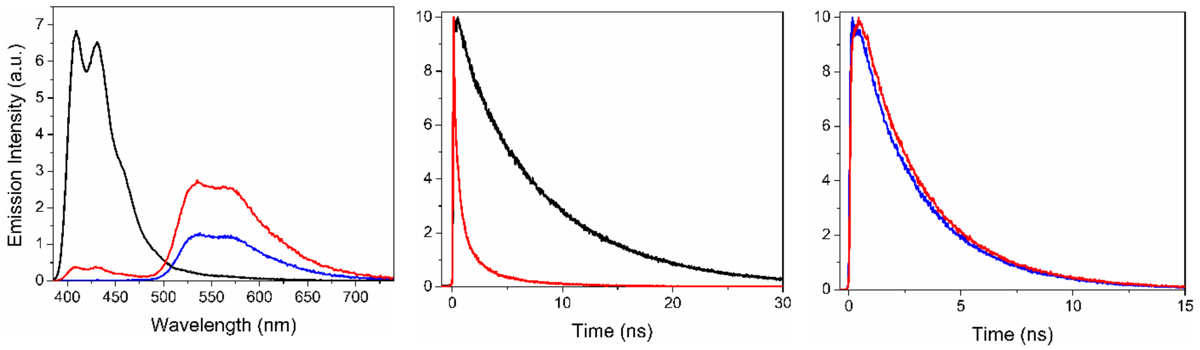

Figure S6. [**DPA**] = 1.8 µM, [**DAEc**] = 1.4 µM.

Decay	A$_1$	τ_1 (ns)	A$_2$	τ_2 (ns)	A$_3$	τ_3 (ns)	τ_{avg} (ns)	χ^2
DPA alone (black)	1291	8.4	276	1.5	-	-	7.2	1.09
DPA cocktail (red)	135	4.3	497	1.0	1101	0.21	0.75	1.17
DAEc alone (blue)	1309	3.1	333	1.2	-	-	2.7	1.0
DAEc cocktail (red)	1287	3.2	460	1.6	-346	0.18	2.8	1.0

($E_{quench, SS}$) = 0.94
($E_{quench, SPC}$) = 0.90
(E_{FRET}) = 0.55

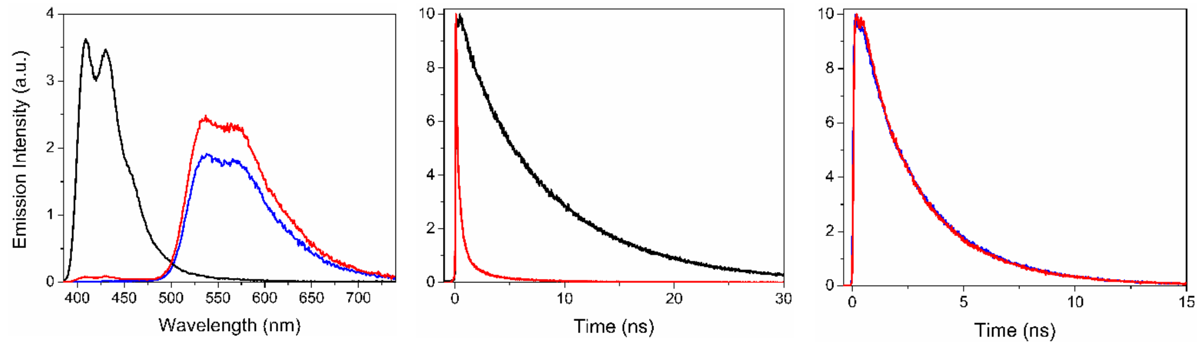

Figure S7. [**DPA**] = 0.9 µM, [**DAEc**] = 2.1 µM.

Decay	A_1	τ_1 (ns)	A_2	τ_2 (ns)	A_3	τ_3 (ns)	τ_{avg} (ns)	χ^2
DPA alone (black)	1316	8.5	250	1.5	-	-	7.4	1.05
DPA cocktail (red)	79	3.4	473	0.62	1462	0.12	0.36	1.16
DAEc alone (blue)	1212	3.1	448	1.2	-	-	2.5	1.02
DAEc cocktail (red)	985	3.1	693	1.5	-	-	2.5	1.18

($E_{quench,\ SS}$) = 0.98
($E_{quench,\ SPC}$) = 0.95
(E_{FRET}) = 0.33

Redox data and driving forces for photoinduced electron transfer (PET) reactions

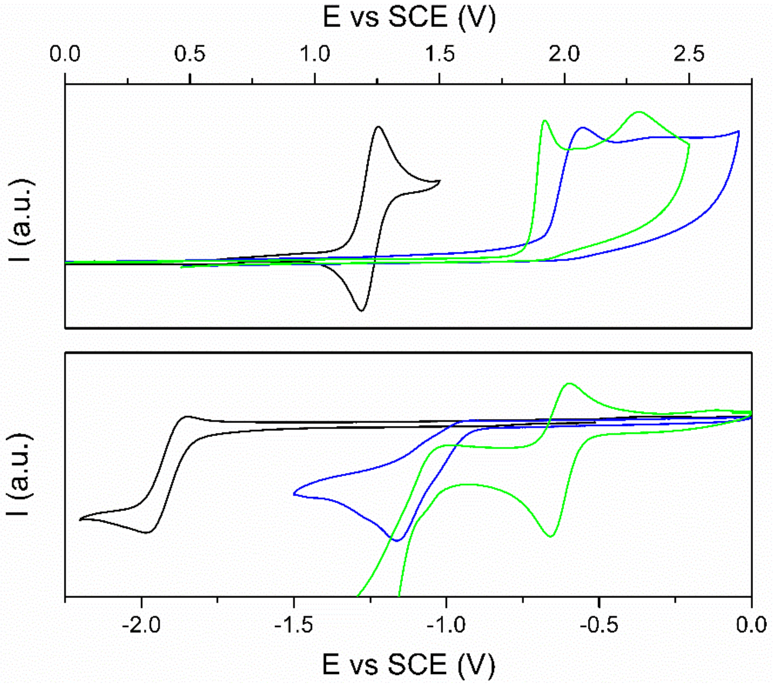

Figure S8. Cyclic voltammograms of **DPA** (black), **DAEo** (blue) and **DAEc** (green) in acetonitrile (+0.1 M of supporting electrolyte). Anodic (oxidation) and cathodic (reduction) scans are shown in the top and bottom panels, respectively.

Listed below are the following parameters:

E_{00} = energy of the lowest excited singlet state

E_{ox} = first oxidation potential (vs SCE)

E_{red} = first reduction potential (vs SCE)

DPA: E_{00} = 3.09 eV (399 nm), E_{ox} = 1.22 V, E_{red} = -1.92 V

DAEo: E_{00} = 3.65 eV (340 nm), E_{ox} = 2.07 V, E_{red} = -1.17 V

DAEc: E_{00} =2.45 eV (506 nm), E_{ox} = 1.92 V, E_{red} = -0.644 V

The corresponding free energy changes (driving forces) for PET were determined using the following equation:

$$\Delta G^0 = e(E_{ox} - E_{red}) - E_{00}$$

Reaction	**ΔG^0 (eV)**
$\mathbf{DPA^{*} + DAEo \rightarrow DPA^{\bullet-} + DAEo^{\bullet+}}$	0.90
$\mathbf{DPA^{*} + DAEo \rightarrow DPA^{\bullet+} + DAEo^{\bullet-}}$	-0.70
$\mathbf{DPA^{*} + DAEc \rightarrow DPA^{\bullet-} + DAEc^{\bullet+}}$	0.75
$\mathbf{DPA^{*} + DAEc \rightarrow DPA^{\bullet+} + DAEc^{\bullet-}}$	-1.2
$\mathbf{DPA + DAEo^{*} \rightarrow DPA^{\bullet-} + DAEo^{\bullet+}}$	0.34
$\mathbf{DPA + DAEo^{*} \rightarrow DPA^{\bullet+} + DAEo^{\bullet-}}$	-1.3
$\mathbf{DPA + DAEc^{*} \rightarrow DPA^{\bullet-} + DAEo^{\bullet+}}$	1.4
$\mathbf{DPA + DAEc^{*} \rightarrow DPA^{\bullet+} + DAEc^{\bullet-}}$	-0.59

Simulations of the donor-acceptor distances in the micelles

As a first estimate of the donor-acceptor intermolecular distances, we performed a basic inter mean-particle distance calculation, given an internal micellar concentration of **DPA** = 8 mM, which resulted in average inter-donor distance (**DPA**-**DPA** distance) of 58 Å. However, having both **DPA** and **DAE** present at different concentrations, and with several potential donor-acceptor pair, the system becomes more complex. Thus, we performed Matlab-based simulations in order to determine the average donor-acceptor distance.

The simulations are based on $n = 10000$ iterations of randomly generated donor and acceptor coordinates distributed in a three-dimensional unit sphere in order to simulate the situation inside the dynamic micelles. These coordinate sets were scaled in accordance with the estimated effective hydrophobic core size of the micelles (10 nm diameter). In the simulations, each micelle contained 3 **DPA** molecules and 2 **DAE** molecules.

All donor-acceptor (**DPA**-**DAE**) distances were calculated, sorted, and the two closest donor-acceptor distances were selected in each iteration. This selection is based on the assumption that any excited state intermolecular reaction (e.g. PET or FRET) most likely will occur with the closer acceptors. Including all possible distances would not properly mirror the actual distance at which the majority of interactions take place. This resulted in an average distance of donor-acceptor interactions of 31 Å. This is to be compared with the calculated Förster radius of 52Å for the **DPA**-**DAEc** FRET pair.

References

(1) K. Uno, H. Niikura, M. Morimoto, Y. Ishibashi, H. Miyasaka, M. Irie, *J. Am. Chem. Soc*. **2011**, *133*, 13558.

(2) I. Yildiz, S. Impellizzeri, E. Deniz, B. McCaughan, J. F. Callan, F. M. Raymo, *J. Am. Chem. Soc.* **2011,** *133*, 871.

(3) K. Suzuki et al., *Phys. Chem. Chem. Phys*. **2009**, *11*, 9850.

(4) K. Rurack, M. Spieles, *Anal. Chem*. **2011**, *83*, 1232.